

Chapter 6

Stacks of Membranes

As we have seen in the previous chapter, the thermal fluctuations of quantum fluid membranes induce a crumpling transition. This effect is mainly due to the extra degree of freedom introduced in the Canham-Helfrich model, namely, the time. A similar phenomenon can be observed in a system of many membranes on top of each other. Although the mathematical description of a stack of membranes appears almost identical to that of a quantum membrane, the physics of the two systems is quite different, as we shall see in this chapter.

Under suitable conditions, lipid membranes in aqueous solution form lamellar structures, characterized by a parallel arrangement of the membranes alternating with thin layers of water [82]. The existence of such structures is in contrast to the behavior of a single tensionless membrane subject to thermal fluctuations, which is always in a disordered, crumpled phase, filling the embedding space completely, as discussed in the previous chapters. In a stack, this phase is suppressed by the steric repulsion between the membranes which prevents them from passing through each other [82], thus constraining the amplitude of the height fluctuations of each membrane to be less than the distance to its nearest neighbors.

The lamellar phase, however, does not always exist, since at sufficiently high temperatures thermal fluctuations can destroy the vertical order [83], as we will see.

Such a transition does not take place in the simplest model of a stack proposed by Helfrich [82], where the membranes possess only a harmonic curvature energy and repulsive term accounting for the vertical forces in the stack, approximating in a rough way the steric repulsion. In this purely

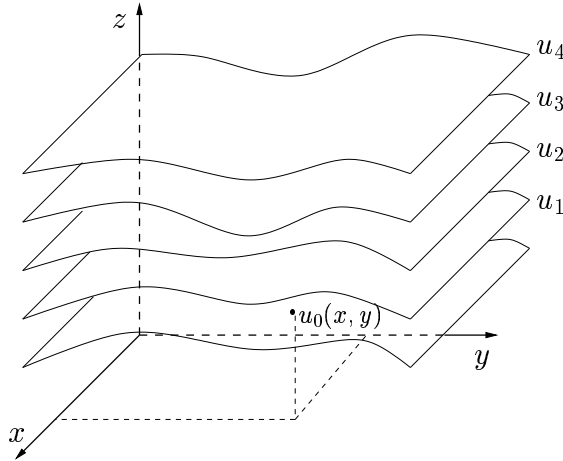


Figure 6.1: Schematic representation of a stack of membranes.

harmonic approximation, the theory is equivalent to de Gennes' theory of smectic-A liquid crystals, having only an ordered phase [84].

6.1 The model

We consider a generalization of the Helfrich model due to Janke and Kleinert [85], in which a multilayer system is made up of $(N+1)$ fluid membranes, parallel to the xy plane of a Cartesian coordinate system, separated a distance l , as shown in Fig. 6.1. If the vertical displacement of the m th membrane with respect to this reference plane is described by a function $u_m(\mathbf{x}) \equiv u(\mathbf{x}_\perp, ml)$, where $\mathbf{x}_\perp = (x, y)$, the energy of the stack reads:

$$E = \sum_m \int d^2x_\perp \sqrt{g_m} \left[r_0 + \frac{1}{2}\kappa_0 H_m^2 + \frac{B_0}{2l}(u_m - u_{m-1})^2 \right]. \quad (6.1)$$

Here, H_m is the mean curvature of the m th membrane, and $g_{m,ij} = \delta_{ij} + \partial_i u_m \partial_j u_m$ the induced metric, with $i, j = 1, 2$, $\partial_1 = \partial/\partial x$, $\partial_2 = \partial/\partial y$ and $g_m = \det[g_{m,ij}]$. The parameter B_0 is the compressibility of the stack.

In the original Helfrich model, the surface tension r_0 was not included because the membranes in the stack are tensionless. We have included r_0 in the energy (6.1), since, as discussed in Chapter 2, it is the *renormalized*

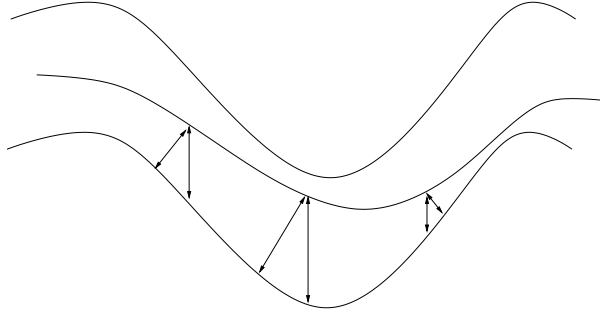


Figure 6.2: The normal gradient term assures that the shortest distance between two neighboring membranes be accounted for when computing the energy (6.2).

surface tension that should be set equal to zero, not the bare one. After carrying out the various integrals, the physical tension will be set equal to zero.

For slow spatial variations, the discrete variable ml may be replaced with a continuous one, and $u(\mathbf{x}_\perp, ml) \rightarrow u(\mathbf{x})$, where $\mathbf{x} = (\mathbf{x}_\perp, z)$. In this limit, the energy (6.1) reduces to

$$E_0 = \int_0^{L_\parallel} dz \int d^2x_\perp \sqrt{g} \left[\sigma_0 + \frac{1}{2} K_0 H^2 + \frac{1}{2} B_0 (\partial_z u)^2 \right]. \quad (6.2)$$

Here we have introduced bulk versions of the surface tension $\sigma_0 \equiv r_0/l$ and bending rigidity $K_0 \equiv \kappa_0/l$, and defined $L_\parallel \equiv Nl$. The vertical gradient energy $(\partial_z u)^2$ should now be replaced by the normal gradient energy $(\mathbf{N} \cdot \nabla u)^2$, which is physically more correct and has the advantage of being reparametrization invariant (see also Ref. [66, 67]). Moreover, the normal distance between neighboring membranes is the relevant one for steric repulsion, as illustrated in Fig. 6.2. In the following, we shall derive all results for both terms and analyze the difference between the two.

6.2 Perturbative calculation

Let us first study the stack perturbatively, starting with the lamellar configuration, and expand the theory in the inverse parameter $\alpha_0 = 1/K_0$, which is assumed to be small. To keep our notation in conformity with the

literature, we use K_0 throughout the text and resort to its inverse only when necessary.

Expanding the energy (6.2) up to fourth order in the displacement field $u(\mathbf{x})$, we arrive at

$$\begin{aligned} E = \int_0^{L_{\parallel}} dz \int d^2x_{\perp} & \left[\frac{1}{2}\sigma_0(\partial_i u)^2 + \frac{1}{2}K_0(\partial_i^2 u)^2 + \frac{1}{2}B_0(\partial_z u)^2 \right. \\ & - \frac{1}{8}\sigma_0(\partial_i u)^2(\partial_j u)^2 - \frac{1}{4}K_0(\partial_i^2 u)^2(\partial_j u)^2 \\ & - K_0(\partial_i u)(\partial_j u)(\partial_i \partial_j u)(\partial_k^2 u) \\ & \left. \pm \frac{1}{4}B_0(\partial_z u)^2(\partial_i u)^2 \right], \end{aligned} \quad (6.3)$$

where the lower sign in the last term refers to the more physical normal gradient energy $(\mathbf{N} \cdot \nabla u)^2$. For zero surface tension, the lowest-order contribution to the energy due to longitudinal displacements is of the usual elastic form $\frac{1}{2}B_0(\partial_z u)^2$, while that due to transverse displacements is of higher order, viz. $\frac{1}{2}K_0(\partial_i^2 u)^2$.

The one-loop contributions are calculated in a derivative expansion. Since the stack is periodic and of finite extent in the z -direction, the Fourier transform includes a sum $(1/L_{\parallel}) \sum_{n=-N/2}^{N/2}$ over the discrete wavevector components

$$\omega_n = \frac{2\pi}{L_{\parallel}} n. \quad (6.4)$$

We take into account the interlayer spacing l in a rough way by restricting the values of the discrete variables to $|\omega_n| < \pi/l$, so that the summation index n lies in the interval $-\frac{1}{2}N < n < \frac{1}{2}N$.

The phase transition we wish to describe is caused by a competition between the softening of the bending rigidity due to thermal fluctuations and the stack-preserving vertical elastic forces. To understand this competition we study how thermal fluctuations renormalize the parameters of the theory. To one-loop order, the bare parameters are renormalized to

$$\sigma_{\text{eff}} = \sigma_0(1 + I_1), \quad K_{\text{eff}} = K_0(1 - \frac{3}{2}I_2), \quad B_{\text{eff}} = B_0(1 \pm \frac{1}{2}I_2), \quad (6.5)$$

where

$$I_1 = \frac{k_B T}{L_{\parallel}} \sum_{n=-N/2}^{N/2} \int \frac{d^2 q_{\perp}}{(2\pi)^2} \frac{\frac{1}{2} \frac{B_0}{\sigma_0} \omega_n^2 - q_{\perp}^2 - \frac{3}{2} \frac{K_0}{\sigma_0} q_{\perp}^4}{B_0 \omega_n^2 + \sigma_0 q_{\perp}^2 + K_0 q_{\perp}^4} \quad (6.6)$$

$$I_2 = \frac{k_B T}{L_{\parallel}} \sum_{n=-N/2}^{N/2} \int \frac{d^2 q_{\perp}}{(2\pi)^2} \frac{q_{\perp}^2}{B_0 \omega_n^2 + \sigma_0 q_{\perp}^2 + K_0 q_{\perp}^4}. \quad (6.7)$$

For ease of notation we dropped the subscript eff from the renormalized parameters. Here, as in the rest of this chapter, renormalized quantities will carry no subscript. We regularize the integrals in the ultraviolet by introducing a sharp transverse wavevector cutoff Λ , as we did in Chapter 5. Actually, the divergent contributions to the above integrals are independent of B_0 . This is due to the discrete nature of the stack. By restricting the values of the discrete wavevectors ω_n to account for the interlayer spacing, as explained above, all divergences proportional to B_0 are suppressed.

The renormalization flow is obtained by integrating out transverse wavevectors in a momentum shell $\Lambda/s < q_\perp < \Lambda$, and subsequently rescaling the coordinates, following Wilson's procedure [68] (for details see Appendix C). We thus obtain,

$$I_1 = \frac{1}{2} I_2 = \frac{1}{4\pi} \frac{k_B T}{L_{\parallel}} \frac{1}{K_0} (N+1) \ln s. \quad (6.8)$$

Since these results are independent of σ , we can safely set the surface tension to zero, thus describing a stack of tensionless membranes, characterized by the two remaining parameters, B and K . Under a rescaling $\mathbf{x}_\perp \rightarrow \mathbf{x}_\perp/s$ of the coordinates in the plane and $z \rightarrow z/s^{z_c}$ along the stack axis, the expansion parameter of perturbation theory $\alpha \equiv 1/K$ scales like $\alpha \rightarrow s^{-z_c} \alpha$, and the compressibility scales like $B \rightarrow s^{4-z_c} B$. Here, z_c allows for the possibility of anisotropic scaling. From Eq. (6.3) with $\sigma = 0$, it follows that $z_c = 2$ in the Helfrich model. Using the above results, one readily generates differential recursion relations to lowest nontrivial order

$$\frac{d\alpha}{d \ln s} = -z_c \alpha + \frac{3}{4\pi} \frac{k_B T}{L_{\parallel}} \alpha^2 (N+1) \quad (6.9)$$

$$\frac{dB}{d \ln s} = (4 - z_c) B \pm \frac{1}{4\pi} \frac{k_B T}{L_{\parallel}} B \alpha (N+1). \quad (6.10)$$

Besides the Gaussian fixed point ($\alpha = 0, B = 0$) which is stable in the infrared, the flow equations also admit a nontrivial, unstable fixed point at

$$\alpha^* = \frac{4\pi}{3} \frac{L_{\parallel}}{k_B T} \frac{z_c}{N+1}, \quad B = 0. \quad (6.11)$$

The latter implies the presence of a phase transition at a critical temperature

$$k_B T_c = \frac{4\pi}{3} \frac{N}{N+1} \frac{l z_c}{\alpha^*}. \quad (6.12)$$

According to Eq. (6.11), the ratio $\kappa^*/k_B T$ for the critical bending rigidity $\kappa^* \equiv l/\alpha^*$ of a single membrane is very small, of the order 0.1. Lipid membranes, on the other hand, have usually bending rigidities of a few units of $k_B T$, thus making it rather unlikely that the melting transition predicted by Eqs. (6.11) and (6.12) be observed experimentally. There exist, however, light scattering measurements on samples of diluted lamellar phases which reveal a significant reduction of the bending rigidity. For some solvents, $\kappa \sim 0.8k_B T$ [86], and the bending modulus K for the stack is found to be two orders of magnitude smaller ($\sim 10^{-13} N$) than the value commonly encountered in smectic systems ($\sim 10^{-11} N$). Since the result (6.11) gives this order of magnitude for the bending rigidity, one may hope that a vertically molten phase might be observed in such extremely dilute smectics. A more important application field of our model also may be systems of oil and water separated by soap films, where the transition carries lamellar phases into microemulsions.

The flow diagram corresponding to the above system of differential equations is shown in Fig. 6.3. For $T < T_c$, the inverse bending rigidity α flows

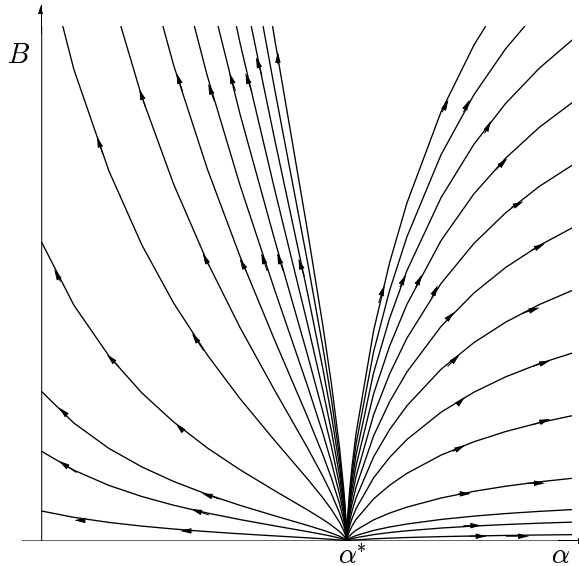


Figure 6.3: Flow diagram in the (α, B) -plane. The diagram is plotted using the lower sign in the last term in Eq. (6.10).

to the Gaussian fixed point at the origin. In this low-temperature phase,

the bending rigidity of the membranes increases with their lateral size, and thermal fluctuations are suppressed. This weak-coupling phase is the lamellar phase, where the translational symmetry is spontaneously broken. For $T > T_c$, on the other hand, α flows with increasing length scales away from the nontrivial fixed point at α^* in the opposite direction. As α increases, the bending rigidity decreases and the membrane fluctuations become stronger. At the critical point α^* , the stack disorders vertically and the system enters a strong-coupling disordered phase. Note that the critical temperature (6.12) depends only weakly on the number ($N + 1$) of membranes.

The flow equations (6.9) and (6.10) can be integrated exactly, yielding:

$$B = c \alpha^{\pm 1/3} \left| \frac{\alpha - \alpha^*}{\alpha} \right|^{4/z_c - 1 \pm 1/3}, \quad (6.13)$$

where c is an integration constant. For $z_c = 2$, the exponent is equal to $1 \pm 1/3$. Explicitly, as we approach T_c from below, B goes to zero as

$$B \sim |T - T_c|^{1 \pm 1/3}. \quad (6.14)$$

The free energy density of the model in the lamellar phase can be calculated in the harmonic approximation, as in Ref. [82]. For a finite stack, it reads

$$f = \frac{1}{16\pi} \frac{k_B T}{L_\parallel^2} \left(\frac{B}{K} \right)^{1/2} N(N+2) \quad (6.15)$$

Thus, as T approaches T_c from below, the free energy density behaves for $z_c = 2$ like

$$f \sim |T - T_c|^{1/2 \pm 1/6}, \quad (6.16)$$

and the specific heat of the stack diverges as

$$C \sim |T - T_c|^{-3/2 \pm 1/6}. \quad (6.17)$$

Figure 6.4 shows a plot of the free energy density and specific heat of the stack for the lower sign in Eqs. (6.16) and (6.17).

We thus see that by using either the vertical gradient energy $(\partial_z u)^2$ or the more physical normal gradient energy $(\mathbf{N} \cdot \nabla u)^2$, the qualitative behavior of the stack of membranes is not altered, but the critical exponents of the melting transition differ from each other. This is due to the fact that the normal gradient energy is zero for the in-plane flow of molecules inside the

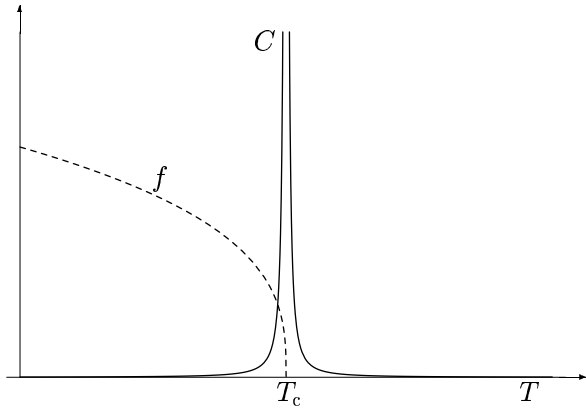


Figure 6.4: Free energy density and specific heat of a stack of membranes, with the lower sign in Eqs. (6.16) and (6.17).

membranes. The vertical gradient energy $(\partial_z u)^2$, on the other hand, includes the energies of the tangential flow. Incompressibility effects have been shown by David [51] and by Kleinert [87] to be irrelevant for the renormalization of a single membrane. Our result implies that this is not the case for a stack of membranes.

The properties of a single membrane are obtained by letting $N \rightarrow 0$ and $z_c \rightarrow 0$. In particular, the flow equation (6.9) of the bending rigidity reduces in this limit to the known result (2.60). It has no fixed point other than the trivial one, which is unstable now, implying that a single membrane is always in the crumpled phase.

6.3 Large- d calculation

By its nature, the perturbative expansion is able to give a satisfactory description only for the ordered phase. For a description of the disordered phase and a better understanding of the entire transition, let us analyze the behavior of a stack of tensionless membranes exactly for very large dimension d of the embedding space. Since the model is exactly solvable in this limit, we can calculate all its relevant properties explicitly, in particular its complete phase diagram as a function of the interlayer separation l .

6.4 The model in large d

For arbitrary d , the vertical displacement of the m th membrane in the stack becomes a $(d - 2)$ -vector field $\mathbf{u}_m(\mathbf{x}_\perp)$. We again consider g_{ij} as an independent field [74], and impose the Monge parametrization metric for each membrane with help of a Lagrange multiplier λ_{ij} . The partition function is a functional integral over all possible configurations $\mathbf{u}_m(\mathbf{x}_\perp)$ of the individual membranes in the stack, as well as over all possible metrics $g_{m,ij}$. After taking again the continuum limit, the partition function reads:

$$Z = \int \mathcal{D}g \mathcal{D}\lambda \mathcal{D}\mathbf{u} e^{-E_0/k_B T}, \quad (6.18)$$

with

$$\begin{aligned} E_0 = \int dz d^2x_\perp \sqrt{g} & \left\{ \sigma_0 + \frac{1}{2}B_0(\partial_z \mathbf{u})^2 + \frac{1}{2}K_0(\partial_k^2 \mathbf{u})^2 \right. \\ & \left. + \frac{1}{2}K_0\lambda^{ij}(\delta_{ij} + \partial_i \mathbf{u} \partial_j \mathbf{u} - g_{ij}) - \frac{1}{4}c_0\lambda_{ii}^2 \right\}, \end{aligned} \quad (6.19)$$

where \mathbf{u} is a $(d - 2)$ -dimensional vector-function of \mathbf{x}_\perp, z . Note that the functional integral over λ in (6.18) has to be performed along the imaginary axis to result in a δ -function. We have introduced a term proportional to λ_{ii}^2 , as in Chapter 5. This term is necessary to renormalize the theory, and its coefficient c_0 corresponds to the large- d in-plane compressibility of the membranes. Since we take the membranes to be incompressible, we shall set the renormalized c equal to zero at the end of our calculations.

The functional integral over \mathbf{u} in Eq. (6.18) is Gaussian and can be carried out to yield an effective energy

$$E_{\text{eff}} = \tilde{E}_0 + E_1, \quad (6.20)$$

with

$$\tilde{E}_0 = \int dz d^2x_\perp \sqrt{g} \left[\sigma_0 + \frac{1}{2}K_0\lambda^{ij}(\delta_{ij} - g_{ij}) - \frac{1}{4}c_0\lambda_{ii}^2 \right], \quad (6.21)$$

and

$$E_1 = \frac{d-2}{2}k_B T \text{Tr} \ln \left[B_0\omega^2 + K_0(q_\perp^4 - q_i\lambda^{ij}q_j) \right], \quad (6.22)$$

where the functional trace Tr is here an integral over space as well as the integral over wavevectors \mathbf{q}_\perp and ω , after replacing $\partial_z^2 \rightarrow -\omega^2$ and $g^{ij}\partial_i\partial_j \rightarrow -\mathbf{q}^2$. Note that the discrete nature of the stack restricts the integral over the wavevectors ω to the first Brillouin zone $|\omega| < \pi/l$.

In the large- d limit, the partition function (6.18) is dominated by the saddle point of the effective energy (6.20) with respect to the metric g_{ij} and the Lagrange multiplier λ^{ij} . For very large membranes, the saddle point can be assumed to be symmetric and homogeneous [76, 77, 78]:

$$g_{ij} = \varrho_0 \delta_{ij}; \quad \lambda^{ij} = \lambda_0 g^{ij} = \frac{\lambda_0}{\varrho_0} \delta^{ij}, \quad (6.23)$$

with constant ϱ_0 and λ_0 . At the saddle point the effective energy (6.20) becomes the free energy of the system.

In the following we shall investigate both the case of an infinite and a finite stack of membranes. As we will see, the large- d approximation allows for the vertical melting even in an infinite stack [88], which is not found perturbatively [82].

6.4.1 Infinite stack

Let us first analyze the case of an infinite stack. To simplify our calculations, we assume the number $N + 1$ of membranes in the stack to be very large, making the distance l between them very small. In this regime, we may extend the limits $\pm\pi/l$ of the integral over ω to infinity. The explicit l -dependence will be introduced later into our calculations.

After evaluating the functional trace in Eq. (6.22), we obtain

$$E_1 = \frac{dk_B T}{2} \int dz d^2x_\perp \varrho_0 \sqrt{\frac{K_0}{B_0}} \left\{ \frac{\Lambda^4}{8\pi} + \frac{\lambda_0}{8\pi} \Lambda^2 + \frac{\lambda_0^2}{64\pi} \left[1 - 2 \ln \left(\frac{4\Lambda^2}{\lambda_0} \right) \right] \right\}, \quad (6.24)$$

where ultraviolet divergences are regularized by introducing a sharp transverse wavevector cutoff Λ and $d - 2$ has been replaced by d for large d .

We may now absorb the first term in (6.24) by renormalizing σ_0 , so that

$$\sigma = \sigma_0 + \frac{dk_B T}{16\pi} \sqrt{\frac{K_0}{B_0}} \Lambda^4 \quad (6.25)$$

is the physical surface tension, which is set equal to zero. The second, quadratically divergent term in (6.24) is used to define the critical temperature as

$$\frac{1}{T_c} \equiv \frac{dk_B}{16\pi} \frac{\Lambda^2}{\sqrt{BK}}. \quad (6.26)$$

The next divergent term, proportional to λ_0^2 , is regularized by introducing a renormalization scale μ and modifying the in-plane compressibility to

$$c = c_0 + \frac{dk_B T}{32\pi} \sqrt{\frac{K_0}{B_0}} \ln \left(4e^{-1/2} \frac{\Lambda^2}{\mu^2} \right). \quad (6.27)$$

The physical in-plane compressibility c is now set equal to zero, as explained in the previous section.

The effective energy thus becomes

$$E_{\text{eff}} = \int dz d^2x_\perp K \lambda \varrho \left\{ \left(\frac{1}{\varrho} - 1 \right) + \frac{T}{T_c} + \frac{aT}{\sqrt{K}} \lambda \left[\ln \left(\frac{\lambda}{\bar{\lambda}} \right) - \frac{1}{2} \right] \right\}, \quad (6.28)$$

with the constants $a \equiv dk_B/64\pi\sqrt{B}$, $\bar{\lambda} \equiv \mu^2 e^{-1/2}$.

From the second derivative matrix of E with respect to ϱ and λ we find that the stability of the saddle point is guaranteed only for $\lambda < \bar{\lambda}$.

Extremizing the above expression with respect to ϱ , we find two solutions for λ , namely $\lambda = 0$ and $\lambda = \lambda_\infty$, with

$$\lambda_\infty \left[\ln \left(\frac{\lambda_\infty}{\bar{\lambda}} \right) - \frac{1}{2} \right] = \frac{\sqrt{K}}{a} \left(\frac{1}{T} - \frac{1}{T_c} \right). \quad (6.29)$$

For $T < T_c$, this equation has no solution for λ_∞ . In this case, the only possible solution is $\lambda = 0$, which corresponds to the ordered phase as we shall verify later. For $T > T_c$, the saddle point lies at $\lambda = \lambda_\infty$, which is now well-defined. This is the vertically disordered phase.

The free energy density at the extremum is given by

$$f = K \lambda_\infty \quad (6.30)$$

and its behavior is similar to the one found perturbatively in Ref. [83]. (see Fig. 6.5).

Extremizing the effective energy (6.28) with respect to λ , we find ϱ as a function of temperature. For $T < T_c$ it is given by

$$\varrho_-^{-1} = 1 - \frac{T}{T_c}. \quad (6.31)$$

This as T approaches T_c from below, indicating the vertical melting at T_c . In the disordered phase, ϱ is found to be

$$\varrho_+^{-1} = \frac{T}{T_c} - 1 - \frac{a\lambda_\infty T}{\sqrt{K}}. \quad (6.32)$$

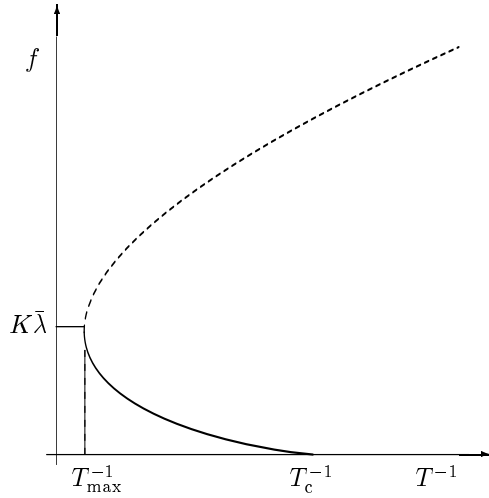


Figure 6.5: Free energy density of an infinite stack of membranes. The dashed curve indicates the unphysical branch of the solution of Eq. (6.29).

As T approaches T_c from above, λ_∞ tends to zero, and ϱ goes again to infinity.

The positivity of ϱ and the stability of the saddle point imply that there is a maximum temperature, given by

$$\frac{1}{T_{\max}} = \frac{1}{T_c} - \frac{a\bar{\lambda}}{\sqrt{K}}, \quad (6.33)$$

below which our assumption that the membranes in the stack are in-plane incompressible does not lead to a stable system.

6.4.2 Finite stack of many membranes

Let us now analyze the case of a finite stack of size L_{\parallel} . Now the functional trace in (6.22) involves a sum over the discrete wavevectors ω_n , given by (6.4). For small λ_0 , a series expansion (see Appendix D.2) leads to

$$E_1 = \int dz d^2\sigma \frac{dk_B T}{2} \varrho_0 e_1, \quad (6.34)$$

with

$$\begin{aligned} e_1 = & \frac{\Lambda^4}{8\pi} \sqrt{\frac{K_0}{B_0}} - \frac{\pi}{12} \sqrt{\frac{B_0}{K_0}} \frac{1}{L_{\parallel}^2} + \frac{\lambda_0}{8\pi} \sqrt{\frac{K_0}{B_0}} \Lambda^2 + \frac{\lambda_0}{4\pi L_{\parallel}} \ln \left(\frac{L_{\perp}^2}{L_{\parallel}} \sqrt{\frac{B_0}{K_0}} \right) \\ & + \frac{\lambda_0^2}{64\pi} \sqrt{\frac{K_0}{B_0}} \left[3 - 2\gamma + 2 \ln \left(\frac{\lambda_0}{8\pi \Lambda^2} \frac{L_{\perp}^2}{L_{\parallel}} \sqrt{\frac{B_0}{K_0}} \right) \right] \\ & + \sqrt{\pi} \sum_{m=3}^{\infty} \frac{(-1)^{m+1} \lambda_0^m}{m 2^{2m} \pi^m} L_{\parallel}^{m-2} \left(\frac{K_0}{B_0} \right)^{\frac{m-1}{2}} \frac{\Gamma(\frac{m-1}{2})}{\Gamma(\frac{m}{2})} \zeta(m-1). \end{aligned} \quad (6.35)$$

As in the case of the infinite stack, we absorb the logarithmic divergence by renormalizing the in plane compressibility via Eq. (6.27), setting c equal to zero for incompressible membranes. The surface tension receives now an L_{\parallel} -dependent renormalization

$$\sigma = \sigma_0 + \frac{dk_B T}{16\pi} \sqrt{\frac{K_0}{B_0}} \Lambda^4 - dk_B T \frac{\pi}{24} \sqrt{\frac{B_0}{K_0}} \frac{1}{L_{\parallel}^2}, \quad (6.36)$$

and σ is again set equal to zero to describe a stack of tensionless membranes.

Extremization of the renormalized combined effective action (6.21) and (6.34) with respect to ϱ leads again to two possible solutions for the saddle point, namely $\lambda = 0$ or $\lambda = \lambda_{L_{\parallel}}$, with

$$\begin{aligned} & \lambda_{L_{\parallel}} \left[\ln \left(\frac{\lambda_{L_{\parallel}}}{\bar{\lambda}} \right) - \frac{1}{2} \right] + \lambda_{L_{\parallel}} \left[1 - \gamma + \ln \left(\frac{L_{\perp}^2}{L_{\parallel}} \frac{1}{8\pi} \sqrt{\frac{B}{K}} \right) \right] \\ & + 32\pi^{3/2} \sum_{m=3}^{\infty} \frac{(-1)^{m+1} \lambda_{L_{\parallel}}^{m-1}}{m 2^{2m} \pi^m} L_{\parallel}^{m-2} \left(\frac{K}{B} \right)^{\frac{m-2}{2}} \frac{\Gamma(\frac{m-1}{2})}{\Gamma(\frac{m}{2})} \zeta(m-1) \\ & = \frac{\sqrt{K}}{a} \left(\frac{1}{T} - \frac{1}{T_{L_{\parallel}}} \right) \end{aligned} \quad (6.37)$$

where

$$\frac{1}{T_{L_{\parallel}}} = \frac{1}{T_c} + \frac{dk_B}{8\pi} \frac{1}{KL_{\parallel}} \ln \left(\frac{L_{\perp}^2}{L_{\parallel}} \sqrt{\frac{B}{K}} \right) \quad (6.38)$$

is the inverse critical temperature for a stack of size L_{\parallel} .

For $T < T_{L_{\parallel}}$, Eq. (6.37) has no solution. In this case, the stack is in the ordered phase, the only available solution for the saddle point being $\lambda = 0$.

For $T > T_{L\parallel}$, there exists a nonzero solution $\lambda_{L\parallel}$, where the system is in the vertically disordered phase.

Let us now examine the saddle point solutions for ϱ . In the vertically disordered phase, where $\lambda = \lambda_{L\parallel}$ is nonzero, we may expand the effective energy in a small- $L\parallel$ series. Extremization with respect to $\lambda_{L\parallel}$ leads to

$$\begin{aligned} \varrho_+^{-1} = & \frac{T}{T_{L\parallel}} - 1 - \frac{a\lambda_{L\parallel}T}{\sqrt{K}} \\ & - \frac{dk_B T}{2K} \sqrt{\pi} \sum_{m=3}^{\infty} \frac{(-1)^{m+1} \lambda_{L\parallel}^{m-1}}{2^{2m} \pi^m} \left(1 - \frac{2}{m}\right) L\parallel^{m-2} \left(\frac{K}{B}\right)^{\frac{m-1}{2}} \\ & \times \frac{\Gamma(\frac{m-1}{2})}{\Gamma(\frac{m}{2})} \zeta(m-1). \end{aligned} \quad (6.39)$$

The positivity of ϱ and the stability of the saddle point again define a maximal temperature, given by

$$\frac{1}{T_{\max}^{L\parallel}} = \frac{1}{T_{\max}} - \frac{dk_B T}{16\pi K L\parallel} \ln \left(\frac{16\pi}{dk_B T_c} \frac{\sqrt{BK}}{\lambda} \right), \quad (6.40)$$

above which our assumption that the membranes in the stack are in-plane incompressible cannot be maintained.

In the ordered phase, the situation is more delicate. For $\lambda = 0$, ϱ can be calculated exactly, and we obtain

$$\varrho_-^{-1} = 1 - \frac{dk_B T}{8\pi K L\parallel} \ln \left[\frac{\sinh \left(\frac{8\pi K L\parallel}{dk_B T_c} \right)}{\frac{L\parallel}{2L_\perp^2} \sqrt{\frac{K}{B}}} \right], \quad (6.41)$$

with an infrared regulator L_\perp equal to the inverse lateral size of the membranes in the stack. If the size $L\parallel$ of the stack is large, (6.41) may be approximated by

$$\varrho_-^{-1} \approx 1 - \frac{T}{T_{L\parallel}}. \quad (6.42)$$

For smaller stacks, however, the positivity of ϱ is not guaranteed. For a fixed, but small stack size $L\parallel$, and for fixed lateral size L_\perp of the membranes in the stack, there is a characteristic temperature defined by

$$T^* = \frac{8\pi K L\parallel}{dk_B \ln(16\pi \sqrt{BK} L_\perp^2 / dk_B T_c)}, \quad (6.43)$$

above which ϱ changes sign, and (6.41) is no longer applicable. Interestingly, for all L_{\perp} and for all finite sizes L_{\parallel} of the stack, the critical temperature $T_{L_{\parallel}}$ is lower than T^* , so that the vertical melting still occurs. The behavior of ϱ is depicted in Fig. 6.6.

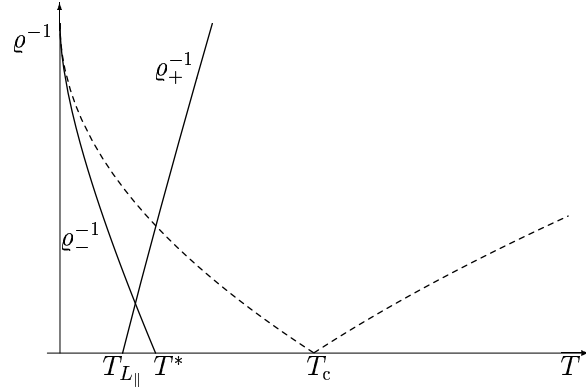


Figure 6.6: Behavior of ϱ^{-1} as a function of T . The solid lines indicate the solutions of the saddle point for ϱ^{-1} for a finite stack. Above $T_{L_{\parallel}}$, ϱ^{-1} is given by (6.39), and below $T_{L_{\parallel}}$ by (6.41). The dashed lines indicate the behavior of ϱ^{-1} for an infinite stack.

Note that Eq. (6.43) reflects the existence of a characteristic horizontal length scale. At fixed temperature $T_{L_{\parallel}} < T < T^*$, and for membranes of lateral size L_{\perp} smaller than

$$L_p = \Lambda^{-1} \exp \left(\frac{4\pi K L_{\parallel}}{dk_B T} \right), \quad (6.44)$$

the height fluctuations of the individual membranes are not strong enough to destroy the ordered phase. The characteristic length L_p corresponds to the de Gennes-Taupin persistence length ξ_p [25] of the individual membranes, below which crumpled membranes appear flat.

6.4.3 Finite number of membranes

Until now we have performed our calculations in the somewhat unphysical continuum approximation, by letting the interlayer separation l be very

small making the number of membranes in the stack very large. Let us now investigate the properties of the stack for a fixed number $N+1$ of membranes at a finite interlayer distance l .

For this purpose, we replace the continuum derivative ∂_z^2 in the z -direction with the discrete gradient operator ∇^2 , whose eigenvalues are given by

$$\nabla^2 g_n = \frac{2(1 - \cos \omega_n l)}{l^2} g_n, \quad (6.45)$$

where g_n is an eigenfunction of ∇^2 . The discrete wavevectors ω_n are now given by

$$\omega_n = \frac{n\pi}{Nl}, \quad n = 1, 2, \dots, N. \quad (6.46)$$

For small interlayer separation l , the free energy is given by (6.34) with

$$\begin{aligned} e_1 = & \frac{\Lambda^4}{8\pi} \sqrt{\frac{K_0}{B_0}} + \frac{1}{Nl^2} \sqrt{\frac{B_0}{K_0}} \\ & + \frac{\lambda_0}{8\pi} \sqrt{\frac{K_0}{B_0}} \Lambda^2 + \frac{\lambda_0}{4\pi Nl} \left[-\ln N + 2N \ln \left(l \sqrt{\frac{K_0}{B_0}} \Lambda^2 \right) \right] \\ & + \frac{\lambda_0^2}{64\pi} \sqrt{\frac{K_0}{B_0}} \left[1 - 2 \ln \left(\frac{4\Lambda^2}{\lambda_0} \right) \right] \\ & + \frac{1}{N\sqrt{\pi}} \sum_{m=2}^{\infty} \frac{(-1)^{m+1} \lambda_0^m}{m 2^{\frac{3m+1}{2}}} l^{m-2} \left(\frac{K_0}{B_0} \right)^{\frac{m-1}{2}} \frac{\Gamma(\frac{m-1}{2})}{\Gamma(\frac{m}{2})} \bar{\zeta}_N(m-1), \end{aligned} \quad (6.47)$$

where we have defined the modified Zeta-function

$$\bar{\zeta}_N(m) = \sum_{n=1}^N \frac{1}{\left[1 - \cos \left(\frac{n\pi}{N} \right) \right]^{\frac{m}{2}}}. \quad (6.48)$$

We proceed by renormalizing the in-plane compressibility via Eq. (6.27), setting c equal to zero for incompressible membranes as before. The surface tension receives an l -dependent renormalization

$$\sigma = \sigma_0 + \frac{dk_B T}{16\pi} \sqrt{\frac{K_0}{B_0}} \Lambda^4 - \frac{dk_B T}{2Nl^2} \sqrt{\frac{B_0}{K_0}} \quad (6.49)$$

and σ is set equal to zero to describe a stack of tensionless membranes, as before. But now the bulk bending rigidity is also modified to

$$K = K_0 - \frac{dk_B T}{4\pi l} \ln \frac{\Lambda^2}{\mu^2}. \quad (6.50)$$

Note that this renormalization agrees with the known result (4.23) for a single membrane.

The saddle point for λ is now given by $\lambda = 0$ or $\lambda = \lambda_l$, with

$$\begin{aligned} \lambda_l \left[\ln \left(\frac{\lambda_l}{\bar{\lambda}} \right) - \frac{1}{2} \right] + 32\sqrt{\pi} \sum_{m=2}^{\infty} \frac{(-1)^{m+1} \lambda_l^{m-1}}{m 2^{\frac{3m+1}{2}}} l^{m-2} \left(\frac{K}{B} \right)^{\frac{m-2}{2}} \\ \times \frac{\Gamma(\frac{m-1}{2})}{\Gamma(\frac{m}{2})} \bar{\zeta}_N(m-1) = \frac{\sqrt{K}}{a} \left(\frac{1}{T} - \frac{1}{T_l} \right) \end{aligned} \quad (6.51)$$

where

$$\frac{1}{T_l} = \frac{1}{T_c} + \frac{dk_B}{8\pi N \kappa} \left\{ -\ln N + 2N \left[\ln \left(l \sqrt{\frac{K}{B}} \bar{\lambda} \right) + \frac{1}{2} \right] \right\} \quad (6.52)$$

is the inverse l -dependent critical temperature, and κ is the bending rigidity of a single membrane in the stack. The two solutions for λ again imply the existence of two different phases, with a phase transition at the critical temperature T_l , which, as in the perturbative case, depends only weakly on the number of membranes in the stack. The corresponding solutions for ϱ , obtained by extremizing the effective energy with respect to λ , are given by

$$\varrho_-^{-1} = 1 - \frac{T}{T_l}, \quad (6.53)$$

for $T < T_l$, that is, in the ordered phase, and

$$\begin{aligned} \varrho_+^{-1} = & \frac{T}{T_l} - 1 - \frac{a\lambda_l T}{\sqrt{K}} \\ & - \frac{dk_B T}{2\sqrt{\pi} NK} \sum_{m=2}^{\infty} \frac{(-1)^{m+1} \lambda_l^{m-1}}{2^{\frac{3m+1}{2}}} \left(1 - \frac{2}{m} \right) l^{m-2} \left(\frac{K}{B} \right)^{\frac{m-1}{2}} \\ & \times \frac{\Gamma(\frac{m-1}{2})}{\Gamma(\frac{m}{2})} \bar{\zeta}_N(m-1), \end{aligned} \quad (6.54)$$

in the vertically molten phase, where $T > T_l$.

The stability of the saddle point requires a minimum interlayer separation

$$l_{\min} = \mu^{-2} \sqrt{\frac{B}{K}} N^{\frac{1}{2N}} \exp \left(\frac{4\pi\kappa}{dk_B T_c} \right) \quad (6.55)$$

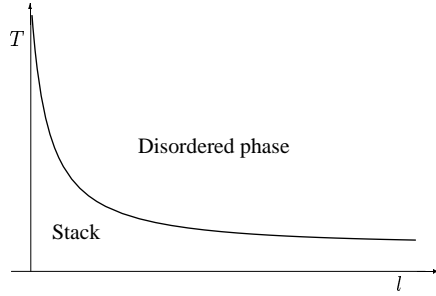


Figure 6.7: Qualitative phase diagram in the $l \times T$ plane. The critical line is plotted for $l > l_{\min}$, for a fixed number $N + 1$ of membranes in the stack. As l increases, the critical temperature T_l goes asymptotically to zero.

below which the stack becomes unstable. l_{\min} is inversely proportional to de Gennes's penetration depth $\sqrt{K/B}$ [89], which is of the order of the interlayer separation in smectic liquid crystals.

The phase diagram of the stack is depicted in Fig. 6.7

6.5 Properties of phases

Let us now characterize both phases in more detail. For temperatures higher than T_l , the solution of the saddle point is $\lambda = \lambda_l$. This corresponds to the disordered phase, where the stack melts. The normals to the membranes are uncorrelated beyond a length scale $\lambda_l^{-1/2}$, as can be derived from the expression for the orientational correlation function, which in the limit $N \rightarrow \infty, l \rightarrow 0$, with constant $Nl = L_{\parallel}$, reads:

$$\langle \partial_i u(\mathbf{x}_{\perp}, z) \partial_j u(\mathbf{x}'_{\perp}, z) \rangle \sim \delta_{ij} e^{-\sqrt{\lambda_l} |\mathbf{x}_{\perp} - \mathbf{x}'_{\perp}|}. \quad (6.56)$$

The length scale $\lambda_l^{-1/2}$ may thus be identified with the persistence length ξ_p [2].

In the low-temperature phase, the solution of the saddle point is $\lambda = 0$. This corresponds to the ordered lamellar phase as can be seen by examining the orientational correlation function in the planes of the membranes. We find in the limit $N \rightarrow \infty, l \rightarrow 0$, with constant $Nl = L_{\parallel}$:

$$\langle \partial_i u(\mathbf{x}_{\perp}, z) \partial_j u(\mathbf{x}'_{\perp}, z) \rangle \sim \frac{\delta_{ij}}{|\mathbf{x}_{\perp} - \mathbf{x}'_{\perp}|^3}. \quad (6.57)$$

This slow, algebraic fall-off of the correlation function implies that, at large distances, the normal vectors to the membranes are still parallel, so that the surfaces remain flat on the average. The effect of thermal fluctuations is suppressed, and they do not disorder the stack.

Another important characteristic is the vertical fluctuation width or roughness ℓ of a membrane in the stack defined by the mean square *height* fluctuation as $\ell^2 = \langle u^2 \rangle$ [90]. In the harmonic approximation, it is given by the one-loop integral

$$\ell^2 = \langle u^2 \rangle = \frac{k_B T}{L_{\parallel}} \sum_{n=-N/2}^{N/2} \int_{1/L_{\perp}}^{\Lambda} \frac{d^2 q_{\perp}}{(2\pi)^2} \frac{1}{B\omega_n^2 + Kq_{\perp}^4}, \quad (6.58)$$

where, in the absence of a surface tension, the largest wavelength is equal to the inverse lateral size $1/L_{\perp}$ of the membranes. As first observed by Peierls and Landau, the mean square fluctuations diverge in the infrared. They thus destroy the long-range *positional* order in the layered system at any finite temperature. More specifically, one finds [90, 89]

$$\ell^2 \sim \frac{k_B T}{2\pi} \left[\frac{L_{\perp}^2}{K L_{\parallel}} + \frac{1}{\sqrt{BK}} \ln(L_{\perp}/a) \right]. \quad (6.59)$$

The first contribution, only present in a finite stack, stems from the $n = 0$ term in the sum in Eq. (6.58). It corresponds to a super soft mode, where the membranes undulate coherently with constant interlayer distance. The second contribution, on the other hand, is also present when the stack is infinite. This contribution increases slowly with the lateral size.

Before proceeding, let us pause for a moment and consider the roughness of the two limiting cases of our theory: a single, tensionless membrane and an infinite, continuum stack of such membranes. In this way, we find

$$\ell^2 = \begin{cases} \int \frac{d^D q_{\perp}}{(2\pi)^D} \frac{k_B T}{\kappa q_{\perp}^4}, & (\text{single membrane}) \\ \int \frac{dq_z d^D q_{\perp}}{(2\pi)^{D+1}} \frac{k_B T}{Bq_z^2 + Kq_{\perp}^4}, & (\text{infinite stack}), \end{cases} \quad (6.60)$$

where instead of a 2-dimensional membrane we consider a D -dimensional object. It follows that for $D > D_u = 4 - z_c$, the roughness is finite in the infrared, indicating that $D_u = 4 - z_c$ is the upper critical dimension. Recall that for a single membrane $z_c = 0$, while for an infinite stack $z_c = 2$. To

determine the lower critical dimension, we consider the mean square normal, or *orientational* fluctuations $\langle (\partial_{\perp} u)^2 \rangle$. This results in an additional factor of q_{\perp}^2 in the numerator of the integrands in (6.60). The resulting expressions are finite in the infrared for $D > D_1 = 2 - z_c$, identifying D_1 as the lower critical dimension. Hence, in going from the limit of a single, tensionless 2-dimensional ($D = 2$) membrane to the opposite limit of an infinite stack, we go from the lower critical dimension of the former to the upper critical dimension of the latter.

Another characteristic of the weak-coupling phase of low-temperature is the behavior of the structure factor

$$S_n(\mathbf{x}) = \langle \exp\{in q_0 [u(\mathbf{x}) - u(0)]\} \rangle, \quad (6.61)$$

where q_0 is parallel to the z -axis, with $|q_0| = 2\pi/l$. This correlation function can be directly observed in X-ray scattering experiments, where the fluctuation spectrum is expressed as half-widths at half-maximum of the anomalous Bragg peaks. As in smectic-A liquid crystals [91, 92], the Fourier transform of the structure factor has algebraic singularities at $q_z = nq_0$:

$$S_n(0, q_z) \sim (q_z - nq_0)^{-2+n^2\eta}, \quad S(q_{\perp}, 0) \sim q_{\perp}^{-4+2n^2\eta}, \quad (6.62)$$

with exponent η . In the harmonic approximation, η can be calculated from Eq. (6.61) and turns out to be the same as for an infinite stack [91]

$$\eta = \frac{k_B T}{8\pi} \frac{q_0^2}{\sqrt{BK}}. \quad (6.63)$$

The algebraic singularities in (6.62) reflect the quasi-long-range periodic order along the stack axis. As for smectic-A liquid crystals, the exponent η is temperature independent. This can be seen by remembering that by simple scaling arguments [82]

$$B \sim \frac{(k_B T)^2}{\kappa} \frac{l}{(l-w)^4}, \quad (6.64)$$

for a stack of membranes of rigidity κ and thickness w . Specifically,

$$\eta \sim \left(1 - \frac{w}{l}\right)^2. \quad (6.65)$$

For smectic-A liquid crystals, this expression was confirmed experimentally [93]. In the high temperature phase, on the other hand, the structure factor $S_n(\mathbf{x})$ behaves, for $z = 0$, like

$$S_n(\mathbf{x}_{\perp}, 0) = \exp(-2n^2\eta\lambda|x_{\perp}|^2), \quad (6.66)$$

revealing the absence of periodic order along the z -axis.

Our system is very similar to a smectic-A liquid crystal, which consists of vertically oriented rod-like molecules layered along the z -axis. Experimentally, the spontaneously broken translational symmetry along this axis and the spontaneously broken rotational symmetry in the layers are restored in a two-step melting process. In the first transition, which can be of first or second order, the smectic melts via dislocation loop unbinding into a translationally disordered nematic. In the second, which is always first order, the orientations of the molecules in the nematic becomes disordered to yield a fully isotropic liquid. If we try to interpret our model as a smectic-A liquid crystal, we see that our vertical melting transition is analogous to the smectic-to-nematic one. The physical mechanism by which our transition takes place, however, is quite different from the dislocation loop unbinding of the defect model. Our membranes cannot split to form dislocations. Instead, they become rough (see Fig. 6.8). This is similar to the two possible ways of representing the superfluid transition in helium: in a defect model, it is explained by a proliferation of vortex lines, whereas in the complex ϕ^4 -theory by a roughening of the order field.

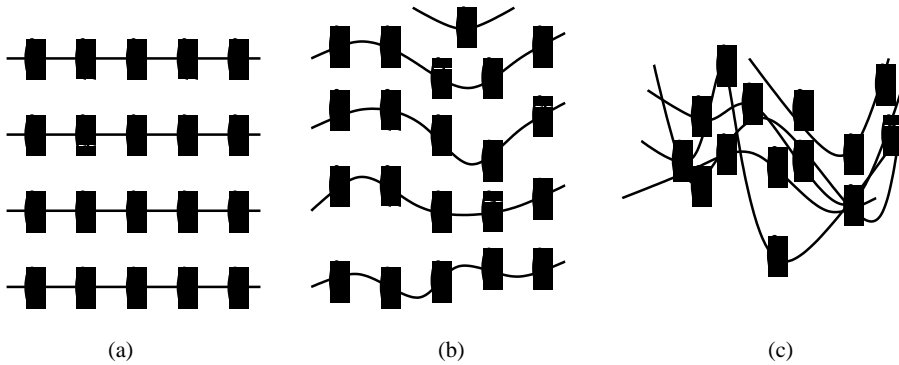


Figure 6.8: Interpretation of the vertical melting of the stack as a smectic-to-nematic phase transition. (a) Smectic-A layers at $T = 0$, (b) Layers at $0 < T < T_l$: still smectic, (c) Interpenetrating rough layers at $T > T_l$: nematic.

Our model does not contain any information about the orientation of the molecules, and is thus unable to describe the second transition. The molecules may be imagined as being attached to the surface in the vertical

direction. The normal vectors to the layered membranes have no relation to the molecule orientation — they are a purely geometrical property of the surfaces.

Let us now calculate the entropy loss in the ordered phase. By a simple scaling argument [82], this quantity should be inversely proportional to the quadratic interlayer spacing,

$$-T\Delta S = \frac{a}{l^2}, \quad (6.67)$$

where a is a temperature-dependent proportionality constant. As we shall see, as the interlayer distance increases, logarithmic corrections must be added to (6.67).

The entropy loss in the ordered phase can be computed by calculating the difference between the free energy density of a single, isolated membrane, and the free energy density of the stack. For small values of λ , it is given by

$$\begin{aligned} -T\Delta S &= \frac{1}{2}\sqrt{\frac{B}{K}} \left(1 + \cot \frac{\pi}{4N}\right) \frac{1}{Nl^2} - \frac{\lambda}{2\pi l} \left(1 - \ln \frac{\lambda l}{2}\sqrt{\frac{K}{B}}\right) \\ &+ \frac{\lambda}{2\pi Nl} \sum_{n=1}^N \ln \sin \frac{n\pi}{2N}. \end{aligned} \quad (6.68)$$

Strictly speaking, the ordered phase corresponds to $\lambda = 0$. In that case, (6.68) agrees with (6.67), and we see no correction to the entropy loss. However, if the size of the membranes in the stack is smaller than the characteristic length L_p , an ordered phase still exists for small values of λ [see discussion after Eq. (6.44)], in which case the corrections to the first term in (6.68) will appear.